Chinese Journal of Chemical Engineering 23 (2015) 1326–1334

Contents lists available at ScienceDirect

Chinese Journal of Chemical Engineering

journal homepage: www.elsevier.com/locate/CJChE

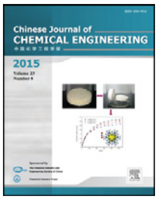

Catalysis, Kinetics and Reaction Engineering

Enhanced performance of g-C_3N_4/TiO_2 photocatalysts for degradation of organic pollutants under visible light☆

Gaixue Song [1], Zhenyu Chu [1], Wanqin Jin [1],*, Hongqi Sun [2],*

[1] State Key Laboratory of Materials-Oriented Chemical Engineering, Nanjing Tech University, Nanjing 210009, China
[2] Department of Chemical Engineering, Curtin University, Perth WA6845, Australia

ARTICLE INFO

Article history:
Received 21 October 2014
Received in revised form 22 April 2015
Accepted 6 May 2015
Available online 14 May 2015

Keywords:
Carbon nitride
Titanium dioxide
Composite
Photodegradation
Sonication

ABSTRACT

Photocatalytic degradation is one of the most promising remediation technologies in terms of advanced oxidation processes (AOPs) for water treatment. In this study, novel graphitic carbon nitride/titanium dioxide (g-C_3N_4/TiO_2) composites were synthesized by a facile sonication method. The physicochemical properties of the photocatalyst with different mass ratios of g-C_3N_4 to TiO_2 were investigated by X-ray diffraction (XRD), scanning electron microscope (SEM), transmission electron microscopy (TEM), N_2 sorption, Fourier transform infrared spectroscopy (FT-IR), X-ray photoelectron spectroscopy (XPS), and UV–vis DRS. The photocatalytic performances were evaluated by degradation of methylene blue. It was found that g-C_3N_4/TiO_2 with a mass ratio of 1.5:1 exhibited the best degradation performance. Under UV, the degradation rate of g-C_3N_4/TiO_2 was 6.92 and 2.65 times higher than g-C_3N_4 and TiO_2, respectively. While under visible light, the enhancement factors became 9.27 (to g-C_3N_4) and 7.03 (to TiO_2). The improved photocatalytic activity was ascribed to the interfacial charge transfer between g-C_3N_4 and TiO_2. This work suggests that hybridization can produce promising solar materials for environmental remediation.

1. Introduction

Over the last few decades, the semiconductor-based photocatalysis has emerged as an environmentally benign technology for wastewater treatment due to its destructive ability towards a wide range of inorganic and organic pollutants [1]. The efficiency of photocatalysis is dramatically dependent on the generation and separation of the photoinduced electron/hole pairs, which are mainly the intrinsic nature of the photocatalyst materials [2]. Many investigations have been implemented on the development of photocatalyst materials, such as metal oxides, sulfides and nitrides, among which titanium dioxide (TiO_2) has demonstrated to be the most popular photocatalyst for potential commercialization [2–5]. TiO_2, an n-type semiconductor, has been then widely used owing to the high efficiency, low cost, non-toxicity and long-term stability [6–9]. However, the large band gap energy of 3.2 eV of TiO_2 (anatase) and the high recombination rate of electron–hole pairs have hindered its wide applications. Many studies have been carried out to improve the visible light absorption and/or separation rate of photoinduced carriers by means of metal or non-metal doping, dye-sensitizing, coupling, surface modification, and semiconductor-coupling [10].

Recently, a novel metal-free photocatalyst, graphite-like carbon nitride (g-C_3N_4) with high thermal and chemical stability together with a moderate band gap energy of 2.7–2.8 eV has demonstrated to be effective for solar energy conversion [11–15]. The delocalized conjugated structure of g-C_3N_4 offers a relatively slow charge recombination rate and a rapid photoinduced charge separation in the electron transfer process, making this material a sensitizer candidate for the design of efficient visible-light-driven photocatalyst [16]. However, due to the low quantum efficiency and high recombination rate of photogenerated electron–hole pairs [17], photocatalytic efficiency of pure g-C_3N_4 is rather low. Moreover, photoreduction capability of g-C_3N_4 is strongly facilitated by the high redox potential of -1.3 V [*vs.* normal hydrogen electrode (NHE) at $\mathrm{pH} = 7$, compared to -0.5 V of TiO_2]. On the other hand, the top energy level of valence band (VB) of g-C_3N_4 is 1.4 V (*vs.* NHE at $\mathrm{pH} = 7$, compared to 2.7 V of TiO_2), resulting in a weak thermodynamical force (oxidative capability) for water oxidation and not enough for producing hydroxyl radicals [18]. As a result, pristine g-C_3N_4 has been rarely used for photodegradation of organic pollutants in water [18–20].

It is expected that coupling TiO_2 with g-C_3N_4 would be able to significantly improve the visible light absorption, carriers' separation, and capability for photooxidation by the created interfaces. Liu *et al.* [21] prepared g-C_3N_4/ZnO hybrid photocatalyst with a higher activity in Rhodamine B (RhB) degradation than either a single phase of ZnO or g-C_3N_4. Ge *et al.* [22] synthesized PANI:g-C_3N_4 by "*in situ*" deposition of oxidative polymerization of aniline monomer in the presence of

---

☆ Supported by the Innovative Research Team Program by the Ministry of Education of China (IRT13070), the Nature Science Foundation of Jiangsu Province (BK2012423, BK20130925), and the Opening Project of State Key Laboratory of Materials-Oriented Chemical Engineering of China (KL13-02).

* Corresponding authors.
E-mail addresses: wqjin@njtech.edu.cn (W. Jin), h.sun@curtin.edu.au (H. Sun).

http://dx.doi.org/10.1016/j.cjche.2015.05.003
1004-9541/

$g\text{-}C_3N_4$ powder. The PANI-$g\text{-}C_3N_4$ composites showed significantly enhanced photocatalytic activities in the MB degradation. Ge *et al.* [23] also prepared MoS_2-$g\text{-}C_3N_4$ *via* a facile impregnation method, and MoS_2-$g\text{-}C_3N_4$ samples demonstrated improved photocatalytic H_2 evolution under visible light irradiations. The 0.5% (by mass) MoS_2-$g\text{-}C_3N_4$ exhibited the highest H_2 evolution rate of 23.10 $\mu mol \cdot h^{-1}$, which was about 11.3 times higher than that of pure $g\text{-}C_3N_4$. Tian *et al.* [24] reported the synthesis of $g\text{-}C_3N_4$-Bi_2WO_6 heterojunctions, and found that the photocatalytic activity in degradation of methyl orange (MO) was almost 3 and 155 times higher than individual C_3N_4 and Bi_2WO_6. Composites of $g\text{-}C_3N_4/Ag_3VO_4$ were prepared by anchoring Ag_3VO_4 to $g\text{-}C_3N_4$, and showed higher activity for basic fuchsin degradation than either Ag_3VO_4 or $g\text{-}C_3N_4$ [25]. He *et al.* [26] reported a novel Z-scheme type MoO_3-$g\text{-}C_3N_4$, which showed an activity in MO degradation 10.4 times higher than $g\text{-}C_3N_4$. WO_3 and Co_3O_4 were also applied to couple with $g\text{-}C_3N_4$ for enhanced photocatalytic activities in degradation of organic pollutants [19,20,27]. For employing the promising properties of TiO_2, the heterojunctions of $g\text{-}C_3N_4/TiO_2$ have attracted particular interests. Chai *et al.* [28] observed an enhanced hydrogen production owing to the synergistic effects by coupling $g\text{-}C_3N_4$ to Pt-TiO_2, such as enhanced light harvesting, improved photostability and efficient photoexcited charge separation. Miranda *et al.* [29] reported that coupling of TiO_2 and $g\text{-}C_3N_4$ can increase the photocatalytic degradation of phenol due to the improved electron–hole separation which results from the appropriate band structures of the composite photocatalyst. Kondo *et al.* [30] developed a highly efficient sulfur-doped TiO_2 hybridized with $g\text{-}C_3N_4$, on which both visible light response and photocatalytic activity in decomposition of acetaldehyde were improved. The catalytic activity of the hybrid was 4 times higher than sulfur-doped TiO_2.

In this study, hydrothermal-induced TiO_2 was hybridized with $g\text{-}C_3N_4$ by a simple sonication procedure with different $g\text{-}C_3N_4$ to TiO_2 mass ratios. The photocatalysts were investigated for photodegradation of MB under UV and visible light, respectively. When $g\text{-}C_3N_4$: TiO_2 was 1.5, the photocatalytic activity in MB degradation was the highest among all the photocatalysts under both UV and visible light irradiations. The synergistic effects of the $g\text{-}C_3N_4/TiO_2$ composites and the enhancements of photocatalytic capacity in the MB degradation process were discussed.

2. Experimental Methods

2.1. Preparation of $g\text{-}C_3N_4$, TiO_2 and $g\text{-}C_3N_4/TiO_2$ hybrid photocatalyst

The polymeric carbon nitride was prepared by a simple thermal condensation method. In a typical synthesis, 2 g melamine was put into an alumina crucible with a cover in order to prevent sublimation of melamine [31], then heated to 520 °C for 4 h in a muffle furnace in air. The synthetic orange-yellow $g\text{-}C_3N_4$ was ground into fine powders and collected for use without further treatment.

TiO_2 nanoparticles were prepared by hydrolysis of titanium tetrachloride ($TiCl_4$) *via* a hydrothermal route. 3.5 ml $TiCl_4$ was firstly added into 40 ml absolute ethyl alcohol. Afterwards, the obtained mixture was placed in a Teflon-lined autoclave. The hydrothermal treatment was performed at 120 °C for 20 h. The produced precipitate was then filtered, washed repeatedly and dried at 80 °C for 6 h. The obtained TiO_2 was ground and collected for further use.

The fabrication process of $g\text{-}C_3N_4/TiO_2$ photocatalysts with various mass ratios ($m_{g\text{-}C_3N_4}$: m_{TiO_2} = 1.1, 1.3, 1.5, 1.7 and 1.9, resulting composites were denoted as $g\text{-}C_3N_4/TiO_2$-1.1, −1.3, −1.5, −1.7 and −1.9, respectively.) was described as follows: certain amount of $g\text{-}C_3N_4$ and TiO_2 were dispersed in absolute ethyl alcohol by vigorously stir for 4 h, followed by a sonication for 60 min at room temperature. After that, the product was collected and dried in an oven at 70 °C for 24 h, and then cooled down to room temperature.

2.2. Characterizations

X-ray diffraction (XRD) was performed on a Rigaku, Miniflex600 X-ray diffractometer, using a Cu K_α radiation (0.15406 nm). The diffraction patterns were recorded from 2θ 10 to 80°. Fourier transform infrared spectra (FT-IR) were recorded on a Nicolet 8700 FT-IR spectrometer using a KBr method. BET surface area and porosity measurements were carried out by N_2 sorption using an ASAP2020 instrument after degassing at 350 °C in vacuum. The UV–visible diffuse reflectance spectra (UV–vis DRS) were obtained on a PerkinElmer Lambda 950 UV–vis spectrometer equipped with an integrating sphere assembly using $BaSO_4$ as the reference sample. The morphologies of samples were investigated by field emission scanning electron microscopy (FESEM S-4800). The samples were dispersed in ethanol using an ultrasonicator and dropped on a copper grid. X-ray photoelectron spectra (XPS) were acquired on Thermo ESCALAB 250 with hemispherical energy analyzer (SPECS) equipped with Al, Ka radiation in the fixed analyzer transmission mode. All peaks in XPS spectra were calibrated by C1s peak at 284.8 eV.

2.3. Photodegradation of methylene blue (MB)

Methylene blue (MB) aqueous solution was used as a model pollutant to evaluate the photocatalytic efficiencies of the samples. The photocatalytic degradation of MB was carried out in a 250 ml reactor at room temperature. The solution volume was 100 ml, the initial concentration of MB solution was 20 $mg \cdot L^{-1}$, and the photocatalyst amount was 1 $g \cdot L^{-1}$. The irradiations were provided by two light sources, UV lamp (2 $mW \cdot cm^{-2}$) and a high pressure Xenon short arc lamp (22.5 $mW \cdot cm^{-2}$) with a filter ($\lambda \geq 400$ nm). The catalyst was magnetically stirred in the dark for reaching the adsorption equilibrium before commencing photocatalytic reaction. After the photocatalytic reaction was initiated by switching on the lamp, MB samples were withdrawn at certain intervals and were filtered for analysis. The solution concentration of MB was determined by a UV–vis spectrophotometer (PerkinElmer Lambda 950).

3. Results and Discussion

3.1. XRD studies

The XRD patterns of TiO_2, $g\text{-}C_3N_4$ and $g\text{-}C_3N_4/TiO_2$ composites are shown in Fig. 1. Two peaks were found from the diffraction pattern of the pristine $g\text{-}C_3N_4$, indicating a typical graphitic structure without any impurity phase [11]. The strong peak at 27.5° represents stacking

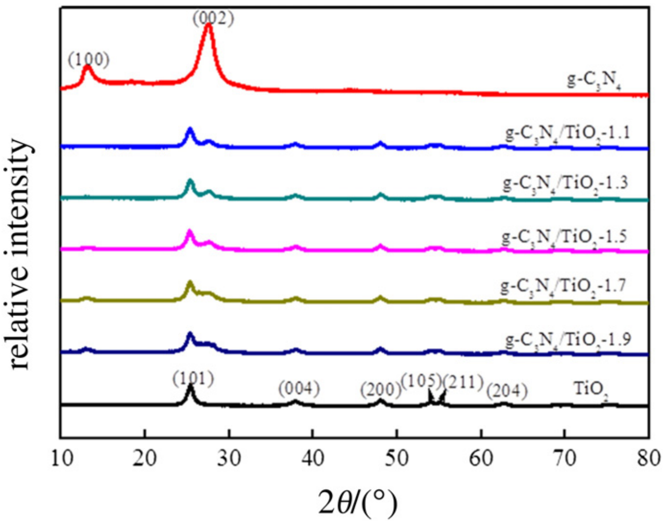

Fig. 1. XRD patterns of pure TiO_2, $g\text{-}C_3N_4$ and $g\text{-}C_3N_4/TiO_2$ composites.